AMERICAN SOCIETY FOR MICROBIOLOGY | Journal of Bacteriology®

RESEARCH ARTICLE

Specific Glucoside Transporters Influence Septal Structure and Function in the Filamentous, Heterocyst-Forming Cyanobacterium *Anabaena* sp. Strain PCC 7120

Mercedes Nieves-Morión,[a] Sigal Lechno-Yossef,[b] Rocío López-Igual,[a]* José E. Frías,[a] Vicente Mariscal,[a] Dennis J. Nürnberg,[c] Conrad W. Mullineaux,[d] C. Peter Wolk,[b] Enrique Flores[a]

Instituto de Bioquímica Vegetal y Fotosíntesis, CSIC and Universidad de Sevilla, Seville, Spain[a]; MSU-DOE Plant Research Laboratory, Michigan State University, East Lansing, Michigan, USA[b]; Department of Life Sciences, Imperial College London, London, United Kingdom[c]; School of Biological and Chemical Sciences, Queen Mary University of London, London, United Kingdom[d]

ABSTRACT When deprived of combined nitrogen, some filamentous cyanobacteria contain two cell types: vegetative cells that fix CO_2 through oxygenic photosynthesis and heterocysts that are specialized in N_2 fixation. In the diazotrophic filament, the vegetative cells provide the heterocysts with reduced carbon (mainly in the form of sucrose) and heterocysts provide the vegetative cells with combined nitrogen. Septal junctions traverse peptidoglycan through structures known as nanopores and appear to mediate intercellular molecular transfer that can be traced with fluorescent markers, including the sucrose analog esculin (a coumarin glucoside) that is incorporated into the cells. Uptake of esculin by the model heterocyst-forming cyanobacterium *Anabaena* sp. strain PCC 7120 was inhibited by the α-glucosides sucrose and maltose. Analysis of *Anabaena* mutants identified components of three glucoside transporters that move esculin into the cells: GlsC (Alr4781) and GlsP (All0261) are an ATP-binding subunit and a permease subunit of two different ABC transporters, respectively, and HepP (All1711) is a major facilitator superfamily (MFS) protein that was shown previously to be involved in formation of the heterocyst envelope. Transfer of fluorescent markers (especially calcein) between vegetative cells of *Anabaena* was impaired by mutation of glucoside transporter genes. GlsP and HepP interact in bacterial two-hybrid assays with the septal junction-related protein SepJ, and GlsC was found to be necessary for the formation of a normal number of septal peptidoglycan nanopores and for normal subcellular localization of SepJ. Therefore, beyond their possible role in nutrient uptake in *Anabaena*, glucoside transporters influence the structure and function of septal junctions.

IMPORTANCE Heterocyst-forming cyanobacteria have the ability to perform oxygenic photosynthesis and to assimilate atmospheric CO_2 and N_2. These organisms grow as filaments that fix these gases specifically in vegetative cells and heterocysts, respectively. For the filaments to grow, these types of cells exchange nutrients, including sucrose, which serves as a source of reducing power and of carbon skeletons for the heterocysts. Movement of sucrose between cells in the filament takes place through septal junctions and has been traced with a fluorescent sucrose analog, esculin, that can be taken up by the cells. Here, we identified α-glucoside transporters of *Anabaena* that mediate uptake of esculin and, notably, influence septal structure and the function of septal junctions.

Received 20 December 2016 **Accepted** 12 January 2017

Accepted manuscript posted online 17 January 2017

Citation Nieves-Morión M, Lechno-Yossef S, López-Igual R, Frías JE, Mariscal V, Nürnberg DJ, Mullineaux CW, Wolk CP, Flores E. 2017. Specific glucoside transporters influence septal structure and function in the filamentous, heterocyst-forming cyanobacterium *Anabaena* sp. strain PCC 7120. J Bacteriol 199:e00876-16. https://doi.org/10.1128/JB.00876-16.

Editor Piet A. J. de Boer, Case Western Reserve University School of Medicine

Address correspondence to Enrique Flores, eflores@ibvf.csic.es.

* Present address: Rocío López-Igual, Institut Pasteur, Unité Plasticité du Génome Bactérien, Département Génomes et Génétique, CNRS, Unité Mixte de Recherche 3525, Paris, France.

KEYWORDS cyanobacteria, glucoside transport, heterocyst, intercellular diffusion, membrane transporters, ABC transporters, major facilitator superfamily

Filamentous cyanobacteria of the orders *Nostocales* and *Stigonematales* fix atmospheric nitrogen in specialized cells called heterocysts (1). Heterocysts are formed from vegetative cells when the filaments of those cyanobacteria lack a source of combined nitrogen (2). The heterocysts provide the vegetative cells with fixed nitrogen, and the vegetative cells, which fix carbon dioxide through oxygenic photosynthesis, provide the heterocysts with reduced carbon (3). Substances exchanged between the two cell types include regulators, such as PatS- and HetN-derived peptides, and nutrients, including amino acids and sugars (4). In the model heterocyst-forming cyanobacterium *Anabaena* sp. strain PCC 7120 (here called *Anabaena*) grown in the absence of combined nitrogen, heterocysts constitute about 10% of the cells and are distributed with a semiregular pattern along the filament (2). This implies that one heterocyst feeds more than one vegetative cell with fixed nitrogen. Two routes have been considered for intercellular molecular transfer, the continuous periplasm of the filament (5, 6) and cell-cell joining structures (7), now termed septal junctions (8–10). The latter would represent a kind of symplasmic route (11) implying intercellular transfer between vegetative cells as well as between heterocysts and vegetative cells.

Proteins SepJ, FraC, and FraD, which are located at the cell poles in the intercellular septa of the filaments of *Anabaena*, are integral membrane proteins (12, 13). SepJ and FraD have predicted extramembrane domains that appear to reside in the periplasm (10, 14–16). Intercellular molecular exchange in the cyanobacterial filament can be traced with fluorescent markers, including calcein, 5-carboxyfluorescein (5-CF), and esculin, and transfer has been found to be impaired in inactivated mutants of *sepJ*, *fraC*, and *fraD* (7, 14, 17, 18). Additionally, perforations (termed nanopores) that have been observed in septal peptidoglycan disks from heterocyst-forming cyanobacteria (19) are present at decreased numbers in those mutants (18). Structures observed by electron tomography of *Anabaena* that have been termed channels (20) likely correspond to the nanopores. SepJ, FraC, and FraD appear to contribute to the formation of cell-cell joining structures (septal junctions) that traverse the septal peptidoglycan through the nanopores. Differential impairment in the transfer of calcein and 5-CF in the *sepJ* and *fraC-fraD* mutants has suggested that two types of septal junction complexes exist, one related to SepJ and another related to FraCD (14).

Sucrose appears to be a quantitatively important metabolite transferred from vegetative cells to heterocysts (21–25). Intercellular transfer of sucrose has been probed in *Anabaena* using esculin (6,7-dihydroxycoumarin β-D-glucoside), a fluorescent analog of this sugar (18). Esculin is taken up into the cells by a mechanism that can be inhibited by the presence of sucrose. Once inside the cells, esculin can be transferred cell to cell in the filament by diffusion through the septal junctions (18, 26). Thus, septal junctions are functionally analogous to the gap junctions of metazoans (18, 26).

In this work, we addressed the transporters that are involved in esculin uptake in *Anabaena* and their role, if any, in intercellular molecular transfer. The genome of *Anabaena* contains several open reading frames (ORFs) predicted to encode components of sugar transporters (27). We have identified three genes that are involved in uptake of esculin, two that encode components of two different ABC uptake transporters and one that encodes a major facilitator superfamily (MFS) transporter. We also found that the three identified glucoside transporters influence intercellular molecular exchange in *Anabaena*. One of the ABC transporter components, an ATP-binding subunit, is needed for the correct subcellular localization of SepJ, and the two other transporters appear to affect SepJ function.

RESULTS

Esculin uptake through α-glucoside transporters. We have previously shown that esculin can be taken up by *Anabaena* filaments grown in BG11 medium (containing

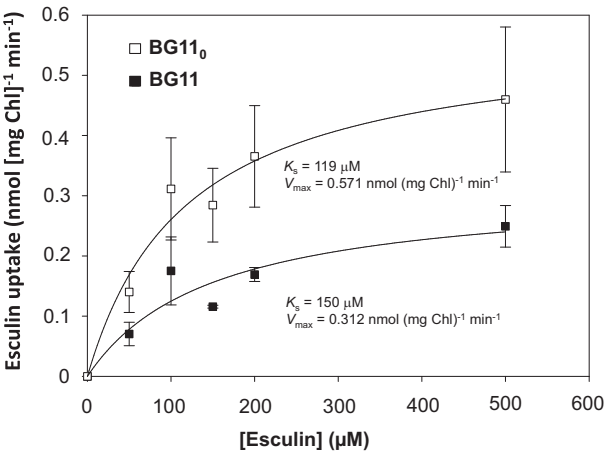

FIG 1 Effect of concentration of esculin on the uptake of esculin by *Anabaena*. BG11-grown filaments or filaments grown in BG11 medium and incubated for 18 h in BG11$_0$ medium were resuspended in the same medium supplemented with 10 mM HEPES-NaOH (pH 7) and used in uptake assays with the indicated concentrations of esculin as described in Materials and Methods. Error bars refer to standard deviations (SD); $n = 3$.

nitrate as the nitrogen source) or grown in BG11 medium and incubated for 18 h in BG11$_0$ medium (lacking any source of combined nitrogen), and that uptake is linear for at least 70 min and takes place at higher levels in the filaments incubated in BG11$_0$ medium (18). To understand better the process of esculin uptake, we determined the dependence of esculin uptake on esculin concentration. Esculin uptake was faster in cells that had been incubated in the absence of nitrate compared to nitrate-grown cultures, with V_{max} values of about 0.31 and 0.57 nmol (mg chlorophyll *a* [Chl])$^{-1}$ min^{-1} for BG11-grown filaments and filaments incubated in BG11$_0$ medium, respectively (Fig. 1). Esculin concentrations giving half-maximal uptake rates (K_s) were 150 and 119 μM in BG11 and BG11$_0$, respectively. Because a concentration somewhat lower than the K_s would permit observation of effects such as competitive or noncompetitive inhibition, we have used 100 μM esculin as a standard concentration in our uptake assays.

The pH dependence of uptake of esculin was investigated. As shown in Fig. 2, the

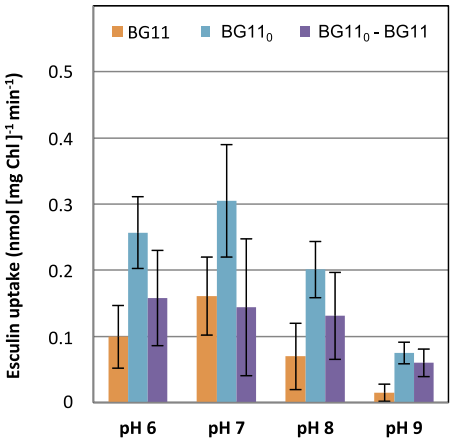

FIG 2 Effect of pH on the uptake of esculin by *Anabaena*. Filaments were grown in BG11 medium and then either were resuspended in BG11 medium or were incubated for 18 h in BG11$_0$ medium and then resuspended in BG11$_0$ medium. Both media were supplemented with 10 mM HEPES-NaOH at the indicated pH values and were used in assays of uptake with 100 μM esculin as described in Materials and Methods. The differences in the mean values of uptake of esculin between filaments resuspended in BG11$_0$ and BG11 at the different pH values tested were represented as BG11$_0$-BG11. Error bars indicate SD. For pH 7, $n = 25$ (BG11) or 20 (BG11$_0$); for all other pH values, $n = 3$.

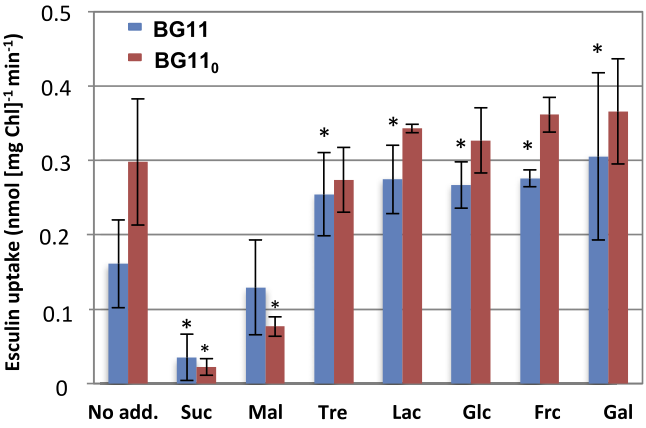

FIG 3 Effect of sugars on the uptake of esculin by *Anabaena*. BG11-grown filaments or filaments grown in BG11 medium and incubated for 18 h in BG11$_0$ medium were resuspended in the same medium supplemented with 10 mM HEPES-NaOH (pH 7) and the indicated sugar at 1 mM. No add., no sugar added; Suc, sucrose; Mal, maltose; Tre, trehalose; Lac, lactose; Glc, glucose; Frc, fructose; Gal, galactose. The assays were performed with 100 μM esculin as described in Materials and Methods. Error bars indicate SD; $n = 2$ to 3, except for the No add. group ($n = 25$ [BG11] or 20 [BG11$_0$]). Asterisks denote significant differences compared to the assays without added sugars in BG11 or BG11$_0$ medium ($P < 0.05$ by Student's t test).

rate of uptake was higher at pH 7 than at lower or higher pH values and was, in every case, higher in filaments incubated in BG11$_0$ medium than in filaments from BG11 medium. The difference in the rate of uptake between filaments from BG11$_0$ and BG11 media decreased as the pH of the assay buffer was increased, suggesting that a H^+-dependent transporter is induced in filaments incubated in BG11$_0$ medium.

Esculin has been used to test the activity of some higher plant sucrose transporters (28) and, consistent with the possibility of uptake through a sucrose transporter(s), inhibition of uptake of esculin by sucrose has been observed in *Anabaena* (18). To characterize further the transporters involved, we tested whether uptake of esculin would be inhibited by various monosaccharides (glucose, fructose, and galactose) and disaccharides (sucrose, maltose, trehalose, and lactose). The results depicted in Fig. 3 show that, in BG11-grown filaments, uptake of esculin was inhibited mainly by sucrose and, to a lesser extent, by maltose. Other sugars tested appear to have stimulated uptake of esculin. In filaments that were incubated in BG11$_0$ medium, inhibition of uptake by sucrose and maltose again was evident. Our results suggest that although esculin is a β-glucoside, its uptake is inhibited mainly by some α-glucosides, sucrose (glucose 1$\alpha\rightarrow$2 fructose) and maltose (glucose 1$\alpha\rightarrow$4 glucose), whereas neither lactose (a β-galactoside; galactose 1$\beta\rightarrow$4 glucose) nor trehalose (a different α-glucoside; glucose 1$\alpha\rightarrow$1α glucose) inhibits uptake of esculin.

Identification of three transporters mediating esculin uptake. Two genes, Ava_2050 and Ava_2748, that encode possible components of ABC uptake transporters for disaccharides or oligosaccharides, are induced in the heterocysts of *Anabaena variabilis* ATCC 29413 (29). BLAST analysis with the genomic sequence of *Anabaena* (30) identified Alr4781 and All0261, with 97% and 99% amino acid identity, respectively, as the products of the *Anabaena* orthologs of those *A. variabilis* genes. Among characterized proteins included in the Transporter Classification Database (TCDB; http://www.tcdb.org), Alr4781 is most similar (45.4% identity, 59.6% similarity; expect, 3.2×10^{-111}) to MalK1, an ATP-binding subunit shared by the glucose/mannose (TCDB no. 3.A.1.1.24) and the trehalose/maltose/sucrose/palatinose (TCDB no. 3.A.1.1.25) transporters from *Thermus thermophilus*, and All0261 is most similar (36.4% identity, 58.9% similarity; expect, 3.3×10^{-51}) to the AraQ permease component of the arabinosaccharide transporter AraNPQ-MsmX from *Bacillus subtilis* (TCDB no. 3.A.1.1.34). We denote *alr4781* as *glsC* and *all0261* as *glsP* (*gls* standing for glucoside). Neither *glsC* nor *glsP* is clustered with other ABC transporter-encoding genes in the *Anabaena* genome.

TABLE 1 Esculin uptake in *Anabaena* and some mutant strains[a]

Strain	Genotype	Product(s) of the mutated gene(s)	Esculin uptake[a] (nmol [mg Chl]$^{-1}$ min^{-1}) in:			
			BG11		$BG11_0$	
			Mean ± SD (*n*)	% of WT (*P*)	Mean ± SD (*n*)	% of WT (*P*)
PCC 7120	WT		0.161 ± 0.059 (25)		0.298 ± 0.085 (20)	
DR3912a	*alr4781*::C.S3	GlsC	0.079 ± 0.037 (10)	49 (0.0003)	0.220 ± 0.065 (9)	74 (0.021)
DR3915	*all0261*::C.S3	GlsP	0.095 ± 0.041 (10)	59 (0.003)	0.217 ± 0.089 (9)	73 (0.027)
DR3912a DR3985a	*alr4781*::C.S3 *all0261*::C.CE	GlsC, GlsP	0.041 ± 0.020 (10)	25 (10^{-6})	0.149 ± 0.024 (5)	50 (0.007)
CSRL15	*alr3705*::pCSRL49	MFS permease	0.181 ± 0.067 (3)	112 (0.591)	0.339 ± 0.073 (4)	113 (0.383)
FQ163	*all1711*::Tn*5*-1063	HepP	0.174 ± 0.076 (4)	108 (0.703)	0.206 ± 0.020 (4)	69 (0.046)
CSMN3	*alr3705*::pCSRL49 *all1711*::Tn*5*-1063	MFS permease, HepP	0.139 ± 0.058 (3)	86 (0.553)	0.200 ± 0.042 (4)	67 (0.037)

[a]Filaments grown in BG11 medium (in the presence of antibiotics for the mutants) were washed and resuspended in BG11 or $BG11_0$ medium without antibiotics and incubated for 18 h under culture conditions. Filaments were then resuspended in the same medium supplemented with 10 mM HEPES-NaOH (pH 7) and used in assays of uptake of 100 μM esculin as described in Materials and Methods. Data are means and SD from the indicated number of assays performed with independent cultures. The significance of the difference between each mutant and the wild type (*P*) was assessed by Student's *t* test.

To test whether the transporters encoded by these *Anabaena* genes can be involved in uptake of esculin, *glsC* was inactivated by insertion of gene cassette C.S3 (31), resulting in *Anabaena* strains that bear the DR3912a mutation (see Fig. S1 in the supplemental material), and *glsP* was inactivated by insertion of C.S3, resulting in *Anabaena* strains that bear the DR3915 mutation, or of C.CE1 (31), resulting in *Anabaena* strains that bear the DR3985a mutation (Fig. S1). BG11-grown filaments of the *glsC* and *glsP* mutants showed esculin uptake activities that were 49% and 59%, respectively, of the wild-type activity (Table 1), and filaments of the *glsC* and *glsP* mutants that had been incubated in $BG11_0$ medium showed 74% and 73%, respectively, of the wild-type activity. Thus, the products of both genes contribute to esculin uptake by *Anabaena* in medium containing nitrate (BG11) and after incubation in medium lacking combined nitrogen ($BG11_0$).

ABC uptake transporters typically comprise one periplasmic solute-binding protein, two integral membrane proteins (transmembrane domains or permeases), and two nucleotide-binding domains that hydrolyze ATP in the cytoplasm (32). If the GlsC ATP-binding subunit and the GlsP permease belong to the same ABC transporter, we would expect that mutation of the two genes would not increase the effect on the uptake of esculin over that of the single mutations. If, on the other hand, GlsC and GlsP belong to two different transporters, we would expect an additive effect of the mutations. A double *glsC glsP* mutant, i.e., an *Anabaena* strain bearing the DR3912a and DR3985a mutations (Fig. S1), showed 25% of the wild-type activity of esculin uptake in BG11-grown filaments and 50% in filaments incubated in $BG11_0$ medium (Table 1), percentages that represent decreased values compared to the effects of the single mutations (49% and 59% for BG11 and 74% and 73% for $BG11_0$). These results suggest that GlsC and GlsP are components of different ABC transporters that can mediate esculin uptake. Notably, significant uptake activity remains in the double mutant, especially in filaments that had been incubated in medium lacking combined nitrogen ($BG11_0$).

Genes *all1711* (*hepP*) and *alr3705* encode predicted MFS proteins that would facilitate movement of disaccharides or oligosaccharides across cell membranes. As shown by results with *all1711*::Tn*5*-1063 mutant strain FQ163 (33), HepP may be a glucoside transporter that is involved in production of the heterocyst-specific polysaccharide layer and may also mediate sucrose transport. According to BLAST analysis, Alr3705 is the predicted *Anabaena* genomic product most similar to higher plant sucrose transporters. *alr3705* was mutated by insertion of C.S3-containing plasmid pCSRL49, producing strain CSRL15, and insertion of pCSRL49 was also combined with *all1711*::Tn*5*-1063 to produce a double mutant, strain CSMN3 (Fig. S2). None of the strains FQ163, CSRL15, or CSMN3, when grown in BG11 medium, was significantly affected in uptake of esculin (*P* values of 0.553 to 0.703 by Student's *t* test), and CSRL15 was not significantly affected when incubated in $BG11_0$ medium (Table 1). In contrast, filaments

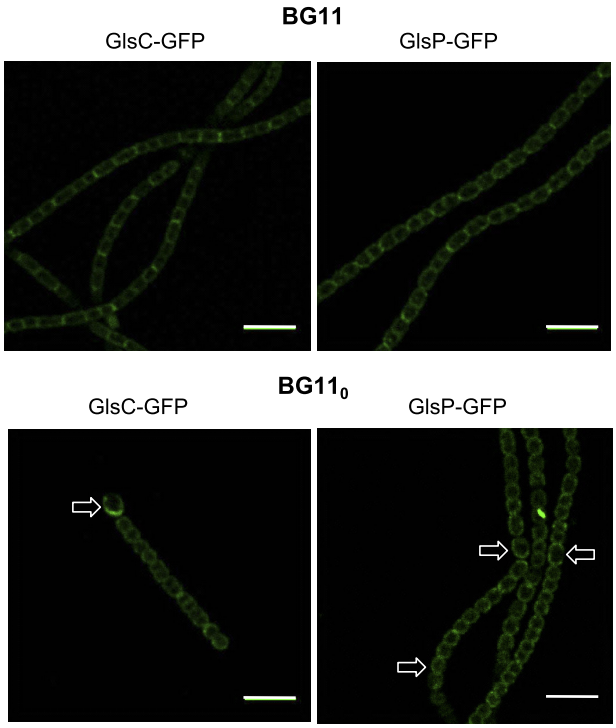

FIG 4 Subcellular localization of GlsC-GFP and GlsP-GFP. Filaments of strains CSMN13 (*glsC*::*gfp*) and CSMN15 (*glsP*::*gfp*) grown in BG11 medium in the presence of antibiotics were incubated in BG11 or $BG11_0$ medium without antibiotics for 24 h. GFP fluorescence was visualized by confocal microscopy as described in Materials and Methods. Brightness and contrast were enhanced to improve visibility. Arrows point to heterocysts. Size bars, 10 μm.

of mutants FQ163 and CSMN3 incubated in $BG11_0$ medium showed similarly decreased activities, 69% and 67% of the wild-type activity, respectively (Table 1). These results indicate that HepP, but not Alr3705, contributed to uptake of esculin in filaments deprived of combined nitrogen.

In conclusion, two ABC transporters, of which GlsC and GlsP are independent components, together are responsible for about 75% and 50% of uptake of esculin in BG11 and $BG11_0$ filaments, respectively, and HepP is responsible for about 30% of uptake of esculin in $BG11_0$ filaments when tested at pH 7. Other transporters therefore should contribute to uptake of esculin in both BG11 and $BG11_0$ media.

Subcellular localization of GlsC and GlsP. To understand better the role of the transporters identified in this work in the physiology of *Anabaena*, we investigated their subcellular localization. The localization of HepP in the cytoplasmic membrane of both vegetative cells and heterocysts has been described previously (33). To study the subcellular localization of GlsC and GlsP, strains producing GlsC-GFP and GlsP-GFP fusion proteins were constructed. As a putative nucleotide-binding domain of an ABC transporter, GlsC is expected to reside in the cytoplasmic face of the cytoplasmic membrane. GlsP is a predicted integral membrane protein that bears six putative transmembrane segments with both the N and C termini in the cytoplasm. Because GFP folds efficiently in the cytoplasm (34), the *gfp-mut2* gene was added to the 3′ end of the *glsC* and *glsP* genes, and the corresponding constructs were transferred to *Anabaena* (Fig. S3). Visualization of filaments of the corresponding strains, CSMN13 (*glsC-gfp*) and CSMN15 (*glsP-gfp*), incubated in BG11 or $BG11_0$ medium showed a relatively low GFP signal that was spread through the periphery of the cells, including the septal regions, where the signal was increased (Fig. 4). Quantification of GFP fluorescence was performed as described in Materials and Methods and is summarized in Fig. S4. The data show that fluorescence was roughly 2-fold higher in the septa than in lateral areas for both GlsC-GFP and GlsP-GFP in cells grown in BG11 medium as well as in cells

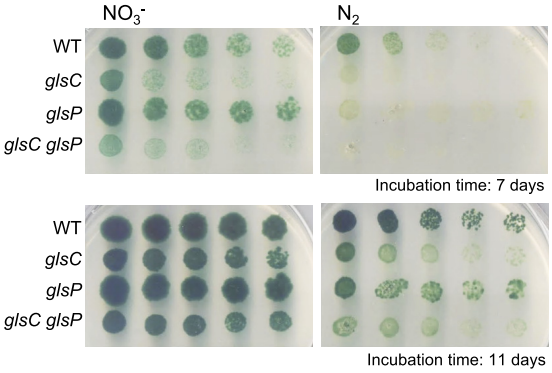

FIG 5 Tests of growth on solid medium of wild-type *Anabaena* and the *glsC* (DR3912a), *glsP* (DR3915), and *glsC glsP* (DR3912a DR3985a) mutants. Filaments grown in BG11 medium (in the presence of antibiotics for the mutants) were resuspended in $BG11_0$ medium, dilutions were prepared, and a 10-μl portion of each dilution (from left to right, 1, 0.5, 0.25, 0.125, and 0.0625 μg Chl ml^{-1}) was spotted on BG11 (NO_3^-) or $BG11_0$ (N_2) medium. The plates were incubated under culture conditions, and photographs taken after 7 and 11 days of incubation are shown to help appreciate the growth defect phenotypes.

incubated in $BG11_0$ medium, indicating that the increased fluorescence from the septa corresponds to the combination of the fluorescence from the adjacent cytoplasmic membranes. Nonetheless, somewhat higher-level GFP fluorescence was observed in septal areas of cells grown in BG11 medium than of cells incubated in $BG11_0$ medium. In filaments incubated in $BG11_0$ medium, the GFP signal was present at similar levels in heterocysts and vegetative cells. These results indicate that GlsC and GlsP are located throughout the cytoplasmic membrane of both vegetative cells and heterocysts. Our results also indicate that levels of GlsC-GFP or GlsP-GFP are generally similar in cells incubated in BG11 and $BG11_0$ media (Fig. S4).

Fox phenotype of the *glsC* and *glsP* mutants. The Fox^- phenotype denotes inability to grow fixing N_2 under oxic conditions, and it is frequently associated with malformation of the heterocyst envelope, as in the case of the *hepP* mutant (33). The growth phenotype was investigated here for the *glsC* and *glsP* mutants. On solid medium, the *glsC* and *glsP* single mutants and the *glsC glsP* double mutant could grow using nitrate or N_2 as the nitrogen source, but the *glsP* mutant showed poorer diazotrophic growth than the wild type, and the *glsC* and *glsC glsP* mutants showed poorer growth in both media (Fig. 5). To determine growth rate constants, growth tests were carried out in liquid medium. In the presence of nitrate (BG11 medium), the growth rate of the single mutants was identical to that of the wild type, whereas the growth rate of the double mutant was 75% of that of the wild type (Table 2). In the absence of combined nitrogen ($BG11_0$ medium), the growth rate of the three mutants was lower than that of the wild type, being especially low in the case of the double mutant (Table 2). Thus, the *glsC*, *glsP*, and *glsC glsP* mutants cannot grow normally fixing N_2 under oxic conditions and therefore show, at best, a weak Fox^+ phenotype. The phenotype of diminished growth of the single mutants could be complemented by introducing in the corresponding mutant a replicative plasmid bearing the wild-type gene, *glsC* or *glsP*; however, when tested on solid medium, complementation was incomplete (Fig. S5). To investigate whether incomplete complementation could result from insufficient expression of the genes in the complemented strains, reverse transcription-quantitative PCR (RT-qPCR) analysis was performed as described in Materials and Methods. Rather than low expression, this analysis indicated 6-fold and 11-fold higher expression of the *glsC* and *glsP* genes, respectively, in the complemented mutants than in the wild type. Therefore, it is possible that overexpression of these genes is deleterious for *Anabaena*.

Production of heterocysts and nitrogenase activity were determined in filaments grown in BG11 medium and incubated for 48 h in $BG11_0$ medium. The *glsC*, *glsP*, and *glsC glsP*

TABLE 2 Growth rates, heterocyst level, and nitrogenase activity in *Anabaena* and ABC transporter mutant strains

Strain (mutated gene[s])	Growth rate constant[a] (day^{-1} [mean ± SD]) (*n*) in:		Heterocysts[b] (%)	Nitrogenase activity[c] (nmol ethylene produced [μg Chl]$^{-1}$ h^{-1} [mean ± SD]) (*n*)	
	BG11	$BG11_0$		Oxic	Anoxic
PCC 7120 (WT)	0.67 ± 0.07 (5)	0.49 ± 0.09 (5)	9.33	23.37 ± 5.17 (4)	10.54 ± 3.05 (3)
DR3912a (*glsC*)	0.67 ± 0.14 (5)	0.28 ± 0.15 (5)	5.58	2.52 ± 1.89 (3)	2.47 ± 0.15 (2)
DR3915 (*glsP*)	0.67 ± 0.07 (5)	0.36 ± 0.08 (5)	7.93	2.13 ± 0.63 (3)	3.00 ± 1.48 (2)
DR3912a DR3985a[d] (*glsC*, *glsP*)	0.50 ± 0.10 (5)	0.06 ± 0.07 (5)	2.22	1.53 ± 1.61 (8)	2.08 ± 1.70 (6)

[a]Growth rate constants (μ) were determined in BG11 or $BG11_0$ liquid medium as described in Materials and Methods for the number of independent cultures shown in parentheses. The difference between the *glsC glsP* mutant and the WT was significant in BG11 ($P = 0.014$ by Student's *t* test) and $BG11_0$ ($P < 0.001$) media; the differences were also significant between *glsC* and WT strains ($P = 0.029$) and between *glsP* and WT strains ($P = 0.045$) in $BG11_0$ medium.

[b]Filaments of the indicated strains grown in BG11 medium (with antibiotics for the mutants) and incubated in $BG11_0$ medium without antibiotics for 48 h were used to determine the percentage of heterocysts (about 1,500 cells were counted for each strain).

[c]Filaments of the indicated strains grown in BG11 medium (with antibiotics for the mutants) and incubated in $BG11_0$ medium without antibiotics for 48 h were used to determine nitrogenase activity. Acetylene reduction was assayed under oxic and anoxic conditions (see Materials and Methods); the differences were significant for all of the mutants versus the WT (*P* values were <0.002 [oxic conditions] and ≤0.05 [anoxic conditions] by Student's *t* test). The number of determinations done with independent cultures is indicated in parentheses.

[d]After 48 h of incubation in $BG11_0$ medium, the filaments of this strain were extensively fragmented (see the text). Those filaments containing heterocysts also contained a mean of 5.4 vegetative cells per filament.

mutants showed about 60%, 85%, and 24%, respectively, of the number of heterocysts observed in the wild type (Table 2). Under oxic conditions, nitrogenase activity was about 10% of the wild-type activity in the two single mutants and about 6.5% in the double mutant (Table 2). Thus, the heterocysts produced in the mutants exhibited low nitrogenase activity. Assay under anoxic conditions showed little or no increase in activity, in contrast to what is normally observed in mutants that bear a defect in the heterocyst envelope (see, for instance, reference 33). The heterocyst envelope-specific polysaccharide layer can be stained with alcian blue, a stain useful to detect bacterial polysaccharides (35). Microscopic inspection of filaments of the *glsC glsP* double mutant stained with alcian blue showed the presence of stained heterocysts, indicating the existence of a polysaccharide layer in the double mutant (Fig. 6). Microscopic inspection also showed that the filaments of the double mutant were very short (Fig. 6). Inspection of cultures of the three mutants showed

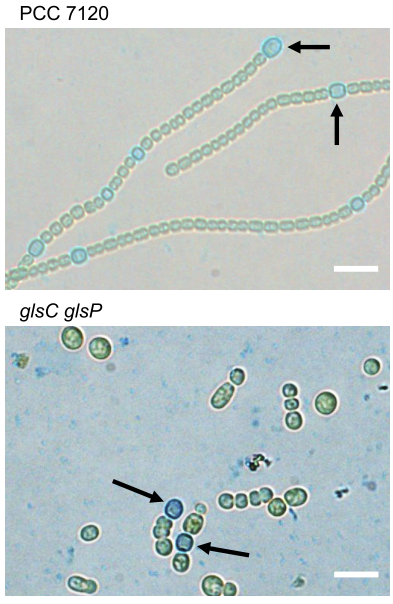

FIG 6 Heterocysts in the *glsC glsP* double mutant. Filaments of the wild type (PCC 7120) and of the double mutant grown in BG11 medium (in the presence of antibiotics for the mutant) were inoculated in liquid $BG11_0$ medium without antibiotics and incubated for 4 days under culture conditions. Staining with alcian blue was done as described in Materials and Methods, and the filament suspensions were observed by light microscopy. Arrows point to some stained heterocysts. Scale bars, 10 μm.

TABLE 3 Transfer of esculin between vegetative cells or from vegetative cells to heterocysts in *Anabaena* and glucoside transporter mutant strains

Strain (mutated gene[s])	Esculin transfer[a] (R [s^{-1}])					
	Vegetative cells in BG11-grown filaments		Filaments incubated in $BG11_0$ medium			
			Vegetative cells		Heterocysts	
	Mean ± SD (n)	% of WT (P)	Mean ± SD (n)	% of WT (P)	Mean ± SD (n)	% of WT (P)
PCC 7120 (WT)	0.157 ± 0.052 (49)		0.162 ± 0.062 (60)		0.060 ± 0.067 (82)	
DR3912a (*glsC*)	0.122 ± 0.051 (77)	78 ($<10^{-3}$)	0.047 ± 0.048 (28)	29 ($<10^{-12}$)	0.074 ± 0.081 (55)	123 (0.277)
DR3915 (*glsP*)	0.144 ± 0.054 (43)	92 (0.200)	0.094 ± 0.077 (25)	58 ($<10^{-4}$)	0.091 ± 0.084 (33)	152 (0.060)
DR3912a DR3985a (*glsC*, *glsP*)	0.105 ± 0.042 (55)	67 ($<10^{-6}$)	0.094 ± 0.070 (37)	58 ($<10^{-5}$)	0.088 ± 0.057 (25)	147 (0.070)
FQ163 (*hepP*)	0.090 ± 0.058 (56)	57 ($<10^{-4}$)	0.068 ± 0.051 (17)	42 ($<10^{-10}$)	0.156 ± 0.082 (27)	260 (10^{-8})

[a]Filaments of the wild type and the indicated mutants grown in BG11 medium (with antibiotics for the mutants) and incubated in BG11 medium without antibiotics for 18 to 24 h or in $BG11_0$ medium without antibiotics for 48 h were used in FRAP analysis as described in Materials and Methods. Data are means ± SD from the results obtained with the indicated number of filaments (n) subjected to FRAP analysis. Filaments from two to six independent cultures were used. The P value, determined by Student's t test (mutant versus wild type), is indicated in each case.

the presence of short filaments in the *glsC glsP* double mutant in both BG11 and $BG11_0$ media, but filament fragmentation was strongest in $BG11_0$ medium (Fig. S6). Such short filaments were not observed in the *glsC* or *glsP* single mutants. Thus, the phenotypic alterations were stronger in the *glsC glsP* double mutant than in the *glsC* or *glsP* single mutants, which is consistent with independent action of the GlsC and GlsP proteins as concluded above from the esculin uptake data.

Intercellular exchange of fluorescent markers. Because the *glsC*, *glsP*, and *hepP* mutants are impaired in glucoside transport and diazotrophic growth, the proteins encoded by these genes could influence intercellular transfer of sucrose. We therefore tested intercellular exchange of esculin in the *glsC*, *glsP*, and *hepP* mutants by means of FRAP (fluorescence recovery after photobleaching) analysis. The results of these tests were analyzed to determine the recovery constant (R) of fluorescence in the cells in which esculin had been bleached (see Materials and Methods and Text S1). To attain adequate labeling of esculin to carry out the FRAP analysis, filaments were incubated for 1 h with 150 μM esculin. Transfer of esculin between vegetative cells of BG11-grown filaments was decreased in a limited way (by about 22%) in the *glsC* mutant but not in the *glsP* mutant (Table 3). However, the effect was larger in the *glsC glsP* double mutant (about 33% inhibition). In the *hepP* mutant, esculin transfer was 43% lower than that in the wild type.

In filaments of the wild type that had been incubated for 48 h in $BG11_0$ medium, esculin transfer between vegetative cells was similar to transfer between BG11-grown vegetative cells, but transfer from vegetative cells to heterocysts was decreased to about 38% of the value between vegetative cells (Table 3). These results are consistent with previously reported data (18). In the mutants, esculin transfer was lower in the $BG11_0$-incubated than in the BG11-grown vegetative cells, and it was especially decreased in the *glsC* mutant (Table 3). In contrast, esculin transfer from vegetative cells to heterocysts was increased in all of the mutants compared to the wild type, and this increase was particularly significant in the *hepP* mutant. In summary, esculin transfer was impaired between vegetative cells of heterocyst-containing filaments but not from vegetative cells to heterocysts.

To assess how specific the effect on intercellular transfer could be, transfer of calcein and 5-CF between nitrate-grown vegetative cells was also tested in the mutants. Calcein transfer was significantly impaired in the three single mutants, and it was lowest (21% of the wild-type activity) in the *glsC glsP* double mutant (Table 4). Transfer of 5-CF was also significantly impaired in the *glsC* and *glsP* mutants, although the effect of the mutations was lower in this case than on calcein transfer, and it was not impaired in the *hepP* mutant. These studies showed that GlsC, GlsP, and HepP are required for normal intercellular molecular exchange in *Anabaena*, but this requirement is more evident when the exchange is tested with calcein than with 5-CF or, as shown above, esculin (compared to BG11-grown filaments).

TABLE 4 Transfer of calcein and 5-CF between nitrate-grown vegetative cells in *Anabaena* and glucoside transporter mutant strains[a]

Strain (mutated gene[s])	Transfer (R [s^{-1}]) of:			
	Calcein		5-CF	
	Mean ± SD (n)	% of WT (P)	Mean ± SD (n)	% of WT (P)
PCC 7120 (WT)	0.070 ± 0.053 (50)		0.087 ± 0.045 (136)	
DR3912a (*glsC*)	0.039 ± 0.033 (47)	55 ($<10^{-3}$)	0.069 ± 0.060 (105)	79 (0.009)
DR3915 (*glsP*)	0.028 ± 0.041 (68)	39 ($<10^{-5}$)	0.059 ± 0.059 (96)	68 ($<10^{-4}$)
DR3912a DR3985a (*glsC*, *glsP*)	0.015 ± 0.020 (43)	21 ($<10^{-8}$)	0.064 ± 0.054 (48)	74 (0.004)
FQ163 (*hepP*)	0.022 ± 0.027 (33)	31 ($<10^{-5}$)	0.082 ± 0.044 (27)	94 (0.604)

[a]Filaments of the wild type and the indicated mutants grown in BG11 medium (with antibiotics for the mutants) and incubated in BG11 medium without antibiotics for 18 to 24 h were used in FRAP analysis as described in Materials and Methods. Data are means ± SD from the results obtained with the indicated number of filaments (n) subjected to FRAP analysis. Filaments from two to six (calcein) or up to 9 (5-CF) independent cultures were used. The P value, determined by Student's t test (mutant versus wild type), is indicated in each case.

SepJ localization and nanopores in the *glsC*, *glsP*, and *hepP* mutants. The fragmentation of filaments observed in the *glsC glsP* double mutant and the effect of the mutation of the glucoside transporters on calcein exchange described above are reminiscent of effects of inactivation of *sepJ* in *Anabaena* (12, 18). We therefore investigated the effect of the inactivation of *glsC*, *glsP*, and *hepP* on the subcellular localization of SepJ. For this investigation, plasmids bearing a *sepJ-gfp* fusion gene were transferred to mutants of those genes, producing strains CSMN9 (*glsC sepJ-gfp*), CSMN10 (*glsP sepJ-gfp*), and CSMN16 (*hepP sepJ-gfp*) (for PCR analysis of the genomic structure of each strain, see Fig. S7). Confocal microscopic inspection of filaments of strains producing SepJ-GFP showed that whereas the *glsP* and *hepP* mutations did not impair SepJ-GFP localization at the intercellular septa, the *glsC* mutation had a strong effect on localization (Fig. 7; for SepJ-GFP localization in four independent clones inspected by fluorescence microscopy, see Fig. S8). In the *glsC sepJ-gfp* strain, spots of

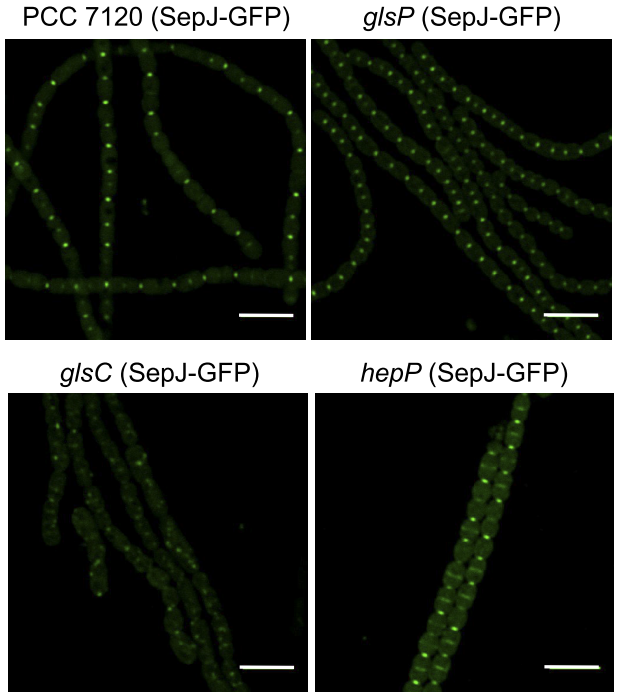

FIG 7 Subcellular localization of SepJ-GFP in the wild-type and transporter mutant genetic backgrounds. Filaments of strains CSAM137 (PCC 7120 [*sepJ*::pCSAM137]), CSMN9 (*glsC*::C.S3 *sepJ*::pCSVT22), CSMN10 (*glsP*::C.S3 *sepJ*::pCSVT22), and CSMN16 (*hepP*::Tn*5*-1063 *sepJ*::pCSAM137) were grown in BG11 medium in the presence of antibiotics and visualized by confocal microscopy as described in Materials and Methods. Size bars, 10 μm. In the *hepP* mutant, SepJ is seen localized in the middle of many cells; these cells are likely starting cell division, and SepJ is known to localize to the cell division site when cell division starts (12, 15).

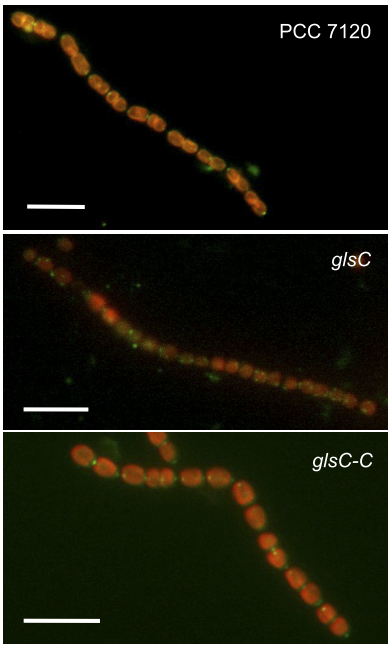

FIG 8 Immunofluorescence localization of SepJ in *Anabaena* (PCC 7120) and the *glsC* and *glsC-C* strains. Filaments of strains PCC 7120, DR3912a (*glsC*::C.S3), and DR3912a(pCSMN22) (*glsC*::C.S3 *glsC*) were grown in BG11 medium in the presence of antibiotics for the mutants and subjected to immunofluorescence analysis with anti-SepJ coiled-coil antibodies as described in Materials and Methods. Overlay images of antibody green fluorescence and cyanobacterial autofluorescence are shown. Size bars, 10 μm.

GFP were only sporadically observed in the center of the septa, and the GFP signal was frequently found throughout the periphery of the cells, including the intercellular septa. Thus, GlsC, but not GlsP or HepP, appears necessary for proper subcellular localization of SepJ.

To corroborate delocalization of SepJ as a result of inactivation of *glsC*, immunolocalization of SepJ was performed using antibodies raised against its coiled-coil domain (17). The antibodies localized SepJ at the cell poles of *Anabaena* (Fig. 8), as previously described (15). In the *glsC* mutant, the signal was largely delocalized, being observed at the cell poles only sporadically. In the complemented *glsC-C* strain [DR3912a(pCSMN22)], SepJ was observed clearly at the cell poles (Fig. 8). These results are fully consistent with the observation that the SepJ-GFP fusion protein shows delocalization of SepJ as the result of inactivation of *glsC* (Fig. 7 and Fig. S8).

Because SepJ is necessary for *Anabaena* to make a normal number of septal peptidoglycan nanopores (18), the number of nanopores was counted in septal peptidoglycan disks observed in murein sacculi isolated from the wild type and the *glsC*, *glsP*, and *hepP* mutants (Fig. 9). Whereas the *glsP* and *hepP* mutants contained a number of nanopores per septum similar to that of the wild type, the septa of the *glsC* mutant contained about 48% of the nanopores found in the wild-type septa.

Protein-protein interactions. The results in the previous section, showing that GlsC is necessary for proper localization of SepJ and formation of septal peptidoglycan nanopores, provides a rationale for understanding the effect of inactivation of *glsC* on the intercellular transfer of calcein, but no effect of inactivation of *glsP* or *hepP* was found. We then studied possible protein-protein interactions involving the glucoside transporters and SepJ using the bacterial adenylate cyclase two-hybrid (BACTH) assay, in which adenylate cyclase activity is reconstituted from two fragments, T25 and T18, of an adenylate cyclase from *Bordetella pertussis* brought together by interacting proteins fused to each of those fragments (36). Reconstituted adenylate cyclase in *Escherichia coli* produces cyclic AMP (cAMP) that promotes induction of *lacZ* encoding

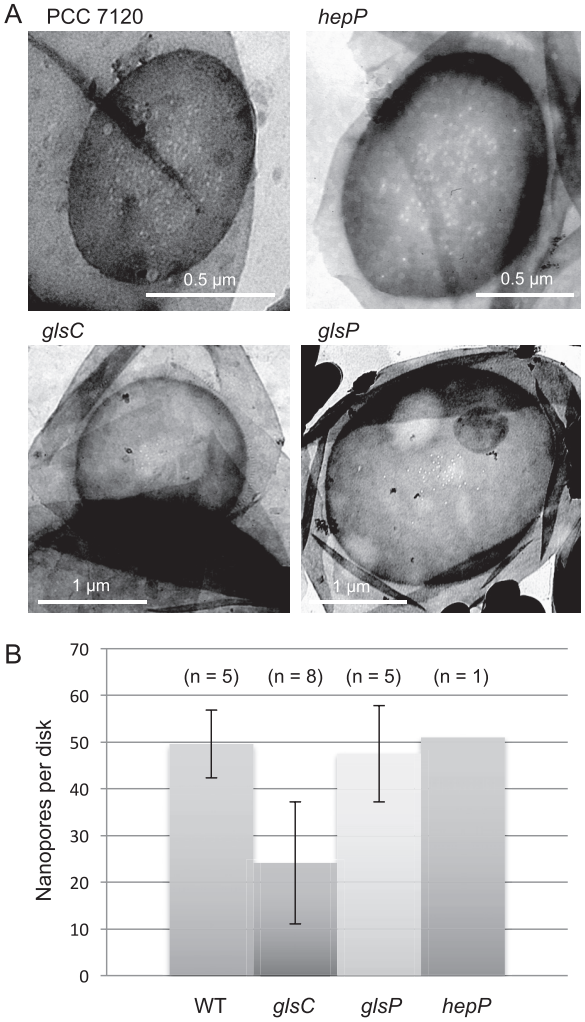

FIG 9 Septal peptidoglycan disk nanopores in wild-type *Anabaena* and mutants. (A) Murein sacculi were isolated from strains PCC 7120 (WT), DR3912a (*glsC*::C.S3), DR3915 (*glsP*::C.S3), and FQ163 (*hepP*::Tn*5*-1063) grown in BG11 medium and visualized by transmission electron microscopy. (B) Quantification of nanopores in disks from the indicated strains (means and SD; *n*, number of disks counted). $P = 0.002$ by Student's *t* test for WT versus *glsC* strains.

β-galactosidase. We have previously shown that SepJ-T25 and SepJ-T18 fusions (where the order of protein names denotes N-terminal to C-terminal orientation) are functional in SepJ self-interactions that produce high β-galactosidase activity (15, 16). As is the case for GlsP, HepP is a predicted integral membrane protein with both the N and C termini in the cytoplasm (33). Because of possible copy number or steric hindrance problems (37, 38), here we tested possible interactions of SepJ-T25 and SepJ-T18 with both N-terminal and C-terminal fusions to T18 and T25, respectively, of each of the glucoside transporter components investigated in this work, GlsC, GlsP, and HepP. The negative control in this analysis was an *E. coli* strain carrying plasmids that produce nonfused T25 and T18 fragments, and additional negative controls producing nonfused T25 or T18 and some of the tested fusions were used. None of these controls produced β-galactosidase activity significantly different from that of the T25/T18 control (Table 5). Combinations of protein fusions involving SepJ that produced β-galactosidase activity significantly higher than the controls included SepJ-T25/SepJ-T18 (positive control), SepJ-T25/T18-HepP, SepJ-T18/T25-HepP, and SepJ-T18/T25-GlsP, but no fusion involving GlsC. These results suggest significant interactions between SepJ and GlsP and, more strongly, between SepJ and HepP. On the other hand, significant interactions were also observed between HepP and GlsP. Finally, HepP self-interactions and GlsC

TABLE 5 Bacterial two-hybrid analysis of protein-protein interactions[a]

Fragment or fusion protein	β-Galactosidase activity (no. of independent transformants) with:							
	T18	SepJ-T18	GlsC-T18	T18-GlsC	GlsP-T18	T18-GlsP	HepP-T18	T18-HepP
T25	12.66 ± 2.34 (9)	10.88 ± 1.06 (6)	13.01 ± 3.49 (4)	12.34 ± 0.80 (4)	12.11 ± 4.10 (4)	10.95 ± 3.37 (4)	12.12 ± 1.33 (4)	11,99 ± 2,69 (4)
SepJ-T25	11.22 ± 2.04 (2)	**80.12 ± 37.03** (9)**	13.25 ± 2.91 (5)	15.75 ± 11.31 (3)	11.74 ± 3.68 (5)	14.66 ± 2.12 (4)	11.42 ± 1.36 (4)	**28.35 ± 5.93** (4)**
GlsC-T25	ND	11.66 ± 1.99 (6)	12.52 ± 3.32 (4)	**20.52 ± 4.90* (4)**	12.36 ± 0.95 (3)	13 ± 5.72 (3)	12.27 ± 3.61 (3)	12.11 ± 1.48 (4)
T25-GlsC	ND	13.09 ± 3.06 (6)	**25.98 ± 5.46** (4)**	15.93 ± 6.35 (6)	12.72 ± 3.11 (4)	12.79 ± 3.73 (3)	13.57 ± 1.92 (4)	11.98 ± 0.86 (4)
GlsP-T25	ND	14.34 ± 2.22 (7)	12.32 ± 3.11 (5)	14.19 ± 7.44 (4)	12.16 ± 2.11 (4)	11.64 ± 4.06 (3)	13.13 ± 2.23 (4)	17.44 ± 4.70 (4)
T25-GlsP	ND	**29.12 ± 9.36** (7)**	11.80 ± 2.27 (5)	15.48 ± 8.28 (4)	11.85 ± 0.55 (3)	12.04 ± 6.11 (3)	13.63 ± 1.47 (4)	**23.08 ± 7.03* (4)**
HepP-T25	10.58 ± 4.35 (4)	12.96 ± 3.26 (4)	12.83 ± 1.50 (4)	12.08 ± 1.12 (4)	13.94 ± 2.29 (4)	13.65 ± 2.48 (4)	13.86 ± 1.37 (4)	16.73 ± 8.38 (4)
T25-HepP	13.60 ± 2.01 (4)	**75.31 ± 6.74** (4)**	14.56 ± 2.47 (4)	13.06 ± 2.81 (4)	18.33 ± 2.50 (4)	**34.16 ± 7.18** (4)**	13.77 ± 0.99 (4)	**79.97 ± 22.12** (4)**

[a]Interactions of T25 and T18 fusion proteins produced in *E. coli* were measured as β-galactosidase activity in liquid cultures. Activity corresponds to nanomoles *o*-nitrophenol (milligrams protein)$^{-1}$ minute^{-1}. The protein fused to the N or the C terminus of T18 or T25 is indicated in each case (N terminus, protein-T18 or protein-T25; C terminus, T18-protein or T25-protein). The means and standard deviations of the results obtained with the indicated number of independent transformants are presented. The difference between each fusion protein combination and the T18/T25 pair was assessed by Student's *t* test; boldface type denotes significant differences
(*, $P \leq 0.005$; **, $P \leq 0.001$). All other combinations gave activities not significantly different from the T25/T18 control ($P > 0.05$). ND, not determined.

self-interactions were also observed, suggesting that HepP and GlsC can form homo-oligomers.

DISCUSSION

Glucoside transporters. Esculin has been successfully used as a fluorescent analog of sucrose to study intercellular molecular exchange in the filaments of *Anabaena* by means of FRAP analysis (18). This analysis requires esculin to be taken up by the cells in the filament, and we have now identified three genes, *glsC*, *glsP*, and *hepP*, that encode components of transporters that mediate esculin uptake in *Anabaena*. The *glsC* (*alr4781*) gene encodes an ATP-binding subunit of an ABC transporter, and the *glsP* (*all0261*) gene encodes an integral membrane (permease) subunit of a different ABC transporter. These genes were investigated because they are the possible *Anabaena* orthologs of genes highly expressed in the heterocysts of a closely related cyanobacterium, *A. variabilis* (29). In *Anabaena*, because the effect of inactivating *glsC* and *glsP* is evident in filaments grown in the presence of nitrate (Table 1), GlsC and GlsP appear to be active in vegetative cells. Additionally, as observed with GFP fusions, GlsC and GlsP are present in heterocysts as well as in vegetative cells (Fig. 4; see also Fig. S4 in the supplemental material). In transcriptomic analysis of *Anabaena*, these genes appear to have low expression, and their expression is not affected by nitrogen deprivation (39). According to the results of inhibition of uptake of esculin by sugars (Fig. 3), the natural substrate of these transporters can be sucrose or an α-glucoside. Sucrose uptake by vegetative cells of *Anabaena* has previously been reported (40), and sucrose transporters that can also transport maltose are frequently found in plants (41). The *Anabaena* glucoside transporters could have a role in the recovery of glucosides from extracellular polysaccharides produced under certain physiological conditions, as has been shown to occur in cyanobacterial mats (42). Consistent with this, biomass of the *glsC* and *glsP* mutants in old BG11 plates is shiny (not shown), which may be indicative of exopolysaccharide accumulation (33). It is also of interest that although *Anabaena* has been considered an obligatory photoautotroph (43), recent data suggest that it can grow using fructose, although this sugar has to be provided at a high concentration unless *Anabaena* is engineered to express a fructose transporter (27, 44). On the other hand, trehalose, lactose, glucose, fructose, and galactose could stimulate esculin uptake (Fig. 3), suggesting that *Anabaena* can use these sugars to support physiological activities such as active transport. As noted earlier, the *Anabaena* genome bears several genes putatively encoding sugar transporters (27), some of which could be involved in the uptake of those sugars.

The third gene that encodes an esculin transporter is *hepP* (*all1711*), which encodes an MFS protein that is also necessary for production of the heterocyst-specific polysaccharide layer (33). We have previously shown that HepP is present at higher levels in developing heterocysts (proheterocysts) and heterocysts than in vegetative cells, and that HepP could mediate sucrose uptake specifically in (pro)heterocysts (33). Because the contribution of HepP to uptake of esculin is evident only in filaments that had been incubated in the absence of combined nitrogen, and because uptake of esculin in these filaments is inhibited by sucrose, HepP may be involved in uptake of sucrose/esculin by (pro)heterocysts. MFS proteins, including sucrose transporters, frequently act as secondary transporters that mediate symport with protons (45). Uptake of esculin that is associated with incubation in $BG11_0$ medium minus uptake in BG11 medium decreases with increasing pH beyond pH 6 (Fig. 2). This observation suggests that a H^+-dependent transporter is induced in filaments incubated in $BG11_0$ medium. Because HepP contributes to esculin uptake associated with incubation in $BG11_0$ medium, our results are consistent with the idea that HepP is a sucrose-H^+ or α-glucoside-H^+ symporter.

Glucoside transporter mutant phenotypes. Inactivation of *hepP* leads to a Fox^- phenotype that has been described in detail (33). We have found that the *glsC* and *glsP* mutants exhibit a weak Fox^+ phenotype: they grow slowly without a source of combined nitrogen under oxic conditions and express low levels of nitrogenase activity

(Table 2). Combination in the same strain of the two mutations, *glsC* and *glsP*, resulted in a greater impairment of diazotrophic growth, very low nitrogenase activity, and a low percentage of heterocysts. Nonetheless, these heterocysts bore an envelope polysaccharide layer (Fig. 6) and their nitrogenase activity was not substantially increased in anoxic assays, suggesting that they do not have a cell envelope problem. To explore the possibility of a limited sucrose supply to the heterocysts, we investigated whether the *glsC* and *glsP* mutations affect intercellular molecular exchange tested with the fluorescent sucrose analog esculin. We have observed that the transfer of esculin in filaments of strains mutated in *glsC*, *glsP*, or *hepP* is impaired between vegetative cells but not from vegetative cells to heterocysts (Table 3). Impairment of sucrose transfer between vegetative cells might eventually limit sucrose supply to heterocysts, and a low supply of reductant would explain the low nitrogenase activities detected in *glsC*, *glsP*, and *glsC glsP* mutants. In the case of the *glsC glsP* double mutant, the small number of vegetative cells in heterocyst-containing filaments, which are short (Fig. 6 and Fig. S6), may further limit the supply of reductant for nitrogenase. On the other hand, esculin transfer to heterocysts was substantially increased in the *hepP* mutant (Table 3). At least some sucrose transporters of the MFS family can function bidirectionally (45), and this could be the case for HepP, which appears to export saccharides from the heterocysts (33). Therefore, the apparently increased transfer of esculin to heterocysts in the *hepP* mutant might reflect increased retention of esculin in the heterocysts of this strain.

Influence of the glucoside transporters on septal junctions. Starting from the observation that the *glsC*, *glsP*, and *hepP* mutants characterized in this work are impaired in the transfer of esculin between vegetative cells, we found that intercellular transfer of fluorescent markers is in general affected in these mutants, with the highest effect being observed on the transfer of calcein. A greater effect on transfer of calcein than of 5-CF or esculin is reminiscent of the effect of inactivation of *sepJ* (14, 17, 18). Hence, these observations suggest a role of the glucoside transporters in proper function of the SepJ-related septal junctions. GFP fusions indicate that GlsC, GlsP, and HepP are located in the periphery of the cells, including the intercellular septa (Fig. 4 and Fig. S4) (33), where they could interact with the septal junction complexes. To investigate whether such interactions are feasible, BACTH analysis was carried out with the glucoside transporter proteins and SepJ. This analysis showed that GlsP and, most strongly, HepP can interact with SepJ, whereas no interaction was observed between SepJ and GlsC. Hence, GlsP and HepP may affect SepJ function by means of protein-protein interactions. A functional dependence between SepJ and an ABC transporter for polar amino acids has also been described (46). These observations suggest that proper operation of SepJ and, hence, of the SepJ-related septal junctions requires interaction with other cytoplasmic membrane proteins.

GlsC is instead required for proper location of SepJ and maturation of the intercellular septa, as illustrated by the presence of a lower number of nanopores in the *glsC* mutant than in the wild type. How GlsC influences SepJ localization and nanopore formation is unknown, but we note (i) that an N-acetylmuramoyl-L-alanine amidase, AmiC, is required for drilling the septal peptidoglycan nanopores (19), and (ii) that the presence of septal proteins, including SepJ, is needed for the amidase to make the nanopores (18). In other bacteria, the ABC transporter-like FtsEX complex, in which FtsE is an ATP-binding subunit, is required for activation of amidases that split the septal peptidoglycan during cell division (47, 48) and of endopeptidases that function in cell elongation (49, 50). An appealing hypothesis is that GlsC participates in an ABC transporter-like complex that regulates amidases involved in nanopore formation with an effect on localization of SepJ.

The different effects of inactivation of *glsC*, i.e., impairment of esculin uptake and alteration of septal structure, indicate that GlsC has multiple functions. Multitask ATP-binding subunits that serve different ABC transporters have been described, e.g., in *Streptomyces lividans* (51), *Streptococcus mutans* (52), *Bacillus subtilis* (53), and *Co-*

rynebacterium alkanolyticum (54), as well as in *Anabaena* (55). As checked at the Integrated Microbial Genomes webpage (https://img.jgi.doe.gov/cgi-bin/m/main.cgi), the *glsC* gene is not clustered with any other gene encoding an ABC transporter component in any cyanobacterium whose genome sequence is available. Therefore, no preferential association of GlsC to any particular ABC transporter can be established based on genomic data. Nonetheless, in a few cases the neighboring genes are related to cell wall biosynthesis, including an N-acetylmuramoyl-L-alanine amidase-encoding gene in *Spirulina major* PCC 6313, consistent with the idea of a relationship between GlsC and cell wall maturation.

In summary, we have identified three genes encoding components of transporters that mediate α-glucoside uptake, including sucrose uptake, in *Anabaena*. These transporters appear to influence septal junction maturation in the case of *glsC* or function in the case of *glsP* and *hepP*. As a consequence, inactivation of these genes impairs molecular transfer between vegetative cells, negatively affecting diazotrophy. A major task for future research is to explore whether the interplay between these transporters and SepJ has a function regulating the activity of septal junctions.

MATERIALS AND METHODS

Strains and growth conditions. *Anabaena* sp. strain PCC 7120 and derivative strains (described in Table S1 in the supplemental material) were grown in BG11 medium modified to contain ferric citrate instead of ferric ammonium citrate (43) or $BG11_0$ medium (BG11 further modified by omission of $NaNO_3$) at 30°C in the light (ca. 25 to 30 μmol photons m^{-2} s^{-1}) in shaken (100 rpm) liquid cultures. For tests on solid medium, medium BG11 or $BG11_0$ was solidified with 1% (wt/vol) Difco Bacto agar. For isolation of the *glsC* (*alr4781*), *glsP* (*all0261*), and *glsC glsP* mutants, *Anabaena* was grown, with shaking, in flask cultures of AA/8 liquid medium with nitrate (56) or in medium AA with nitrate solidified with 1.2% (wt/vol) purified (Difco) Bacto agar (56) at 30°C and illuminated as described above. When appropriate, antibiotics were added to the cyanobacterial cultures at the following concentrations: in liquid cultures, streptomycin sulfate (Sm), 2 to 5 μg ml^{-1}; spectinomycin dihydrochloride pentahydrate (Sp), 2 to 5 μg ml^{-1}; erythromycin (Em), 5 μg ml^{-1}; and neomycin sulfate (Nm), 5 to 25 μg ml^{-1}; in solid media, Sm, 5 to 10 μg ml^{-1}; Sp, 5 to 10 μg ml^{-1}; Em, 5 to 10 μg ml^{-1}; and Nm, 30 to 40 μg ml^{-1}. Chlorophyll *a* (Chl) content of cultures was determined by the method of Mackinney (57).

E. coli strains were grown in LB medium, supplemented when appropriate with antibiotics at standard concentrations (58). *E. coli* strain DH5α or DH5αMCR was used for plasmid constructions. *E. coli* strain DH5α or ED8654, bearing a conjugative plasmid, and strain HB101 or DH5αMCR, bearing a methylase-encoding helper plasmid and the cargo plasmid, were used for conjugation with *Anabaena*, unless stated otherwise (59).

Construction of *Anabaena* mutant strains. The *alr4781* (*glsC*) mutant, DR3912a, was generated by a diparental mating between *Anabaena* and DH5αMCR carrying pRL443, pRL3857a, and pRL3912a (plasmids described in Table S1). The single recombinant was selected on Em, tested for sucrose sensitivity, and then went through a sucrose selection cycle, as described by Cai and Wolk (60), for selection of the double recombinant (Fig. S1). Similarly, an *all0261* (*glsP*) double recombinant deletion mutant, DR3915 (Fig. S1), was generated by mating between *Anabaena* and DH5αMCR carrying pRL443, pRL3857a, and pRL3915. Because DR3912a and DR3915 carry the same antibiotic resistance marker (Sm^r Sp^r), a new plasmid, pRL3985a, was constructed for creation of the *glsC glsP* double mutant (Fig. S1). In this case, pRL3985a was introduced into DR3912a by conjugation, and the mutant was selected as described above.

For complementation of the *glsC* mutant (DR3912a), a fragment containing ORF *alr4781* and 202 bp of upstream and 49 bp of downstream DNA was amplified using *Anabaena* DNA as the template and primers alr4781-3 and alr4781-4 (oligodeoxynucleotide primers are described in Table S1). The PCR product was cloned into vector pSpark I, producing pCSMN21. This construct was verified by sequencing and transferred as a BamHI fragment to pRL25C (61) digested with the same enzyme, producing pCSMN22. This plasmid was transferred to DR3912a by conjugation. Clones resistant to Sm, Sp, and Nm were isolated and their genetic structure verified by PCR with primers alr4781-3 and alr4781-4 (Fig. S5). This strain was named CSMN11. For complementation of the *glsP* mutant (DR3915), a fragment containing ORF *all0261* and 103 bp of upstream and 40 bp of downstream DNA was amplified using *Anabaena* DNA as the template and primers all0261-3 and all0261-4. The PCR product was cloned into pSpark I, producing pCSMN19, which was confirmed by sequencing and transferred as a BamHI fragment to pRL25C digested with BamHI, producing pCSMN20. This plasmid was transferred to DR3915 by conjugation. Clones resistant to Sm, Sp, and Nm were insolated and their genetic structure was verified by PCR with primers all0261-3 and all0261-4 (Fig. S5). This strain was named CSMN12.

For inactivation of *alr3705*, an internal fragment of 560 bp was amplified by PCR using *Anabaena* DNA as the template and primers alr3705-1 (bearing a BamHI site in its 5′ end) and alr3705-2. The amplified fragment was cloned into pMBL-T (http://www.molbiolab.es/uploads/phpgSgmue.pdf; Dominion MBL, Spain) and transferred as a BamHI-ended fragment (the second BamHI site is from the vector multiple-cloning site) to BamHI-digested pCSV3 (62), producing pCSRL49. This plasmid was transformed into *E. coli* HB101 carrying pRL623 and transferred to *Anabaena* and to *hepP* (*all1711*) mutant strain FQ163 (33) by

conjugation with selection for Sm^r and Sp^r (because FQ163 is itself Nm^r, Sm^r, and bleomycin resistant, in this case effective selection is only for Sp^r). Clones that had incorporated pCSRL49 by single recombination were selected for further study and named strain CSRL15 (wild-type background) and CSMN3 (*hepP* background) (Fig. S2).

To prepare an *Anabaena* strain producing a fusion of GFP to GlsC, a 950-bp DNA fragment from the 3′ region of *glsC* (*alr4781*) was amplified using *Anabaena* DNA as the template and primers alr4781-5 and alr4781-6. The 950-bp PCR product was cloned into pSpark I, producing pCSMN23. This construct was validated by sequencing and transferred to SacI-XhoI-digested pRL277 (63) as a SacI-NheI fragment together with NheI-SalI-digested *gfp-mut2* (64), producing pCSMN24, in which the *gfp-mut2* gene is fused to *glsC*. pCSMN24 was transferred to *Anabaena* by conjugation. Clones resistant to Sm and Sp were selected and their genetic structure was verified by PCR with primer pairs alr4781-3/gfp-5 and alr4781-3/alr4781-4. This strain was named CSMN13 (Fig. S3). To prepare an *Anabaena* strain producing a fusion of GFP to GlsP, a 482-bp DNA fragment from the 3′ region of *glsP* (*all0261*) was amplified using *Anabaena* DNA as the template and primers all0261-6 and all0261-5. The PCR product, a SacI-NheI fragment, was inserted together with NheI-SalI-digested *gfp-mut2* into SacI-XhoI-digested pRL277 (63), producing pCSMN25, which bears a fusion of the *all0261* coding sequence to the *gfp-mut2* gene. This construct was verified by sequencing and transferred to *Anabaena* by conjugation. Clones resistant to Sm and Sp were isolated, and integration of the *glsP-gfp* construct was verified by PCR using primer pairs all0261-4/gfp-5 and all0261-3/all0261-4. This strain was named CSMN15 (Fig. S3).

To study the effect of inactivation of transporter genes on the localization of SepJ-GFP, Nm^r plasmid pCSVT22, bearing *sepJ-gfp* (13), was transferred to strains DR3912a (*alr4781*::C.S3) and DR3915 (*all0261*::C.S3) by conjugation. Similarly, the Sm^r Sp^r plasmid pCSAM137, bearing *sepJ-gfp* (12), was transferred to FQ163 (*hepP*::Tn*5*-1063) (33). The genetic structure of selected clones bearing *sepJ-gfp* fusions was studied by PCR with DNA from those clones and primer pair alr2338-3/gfp-5 to test recombination in the correct genomic location (*sepJ*). We also verified the mutant background in the exconjugants using the following primer pairs: for *alr4781*, alr4781-3/alr4781-4; for *all0261*, all0261-3/all0261-4; and for *hepP*, all1711-3/all1711-4 (Fig. S7). Clones bearing the *sepJ-gfp* fusion were named strain CSMN9 (*alr4781* background), CSMN10 (*all0261* background), and CSMN16 (*hepP* background).

RT-qPCR. For RT-qPCR, RNA was isolated as described previously (33) from 50 to 100 ml of shaken *Anabaena* cultures. RNA was treated with Ambion TURBO DNA-free DNase according to the manufacturer's protocol. Three independent RNA samples were analyzed from each strain (the wild type and the complemented *glsC* and *glsP* strains), and three technical replicates were carried out for each sample. RNA (200 ng) was reverse transcribed using a QuantiTect reverse transcription kit (Qiagen) with random primers as indicated by standard protocols of the manufacturer. Quantitative real-time PCR was performed on an iCycler iQ real-time PCR detection system equipped with the iCycler iQ v 3.0 software from Bio-Rad. PCR amplification was performed in a 20-μl reaction mix according to standard protocols of the SensiFAST SYBR and fluorescein kit (Bioline). qPCR conditions were the following: 1 cycle at 95°C for 2 min, followed by 30 cycles of 95°C for 15 s, 67.5°C for 20 s, and 72°C for 30 s. PCR products were checked by a single-peak melting curve. The threshold cycle (C_T) of each gene was determined and normalized to those of reference genes *ispD* (*all5167*) and *dxs* (*alr0599*) to obtain ΔC_T values from each sample. Relative gene expression was calculated using the $2^{-\Delta\Delta CT}$ method (65), and the data presented correspond to the average of data obtained with each reference gene. The following primer pairs were used: all0261-11/all0261-12, alr4781-9/alr4781-10, all5167-1/all5167-2, and alr0599-1/alr0599-2 (Table S1).

Uptake of esculin. *Anabaena* strains grown in BG11 medium, with antibiotics for the mutants, were harvested by centrifugation, washed three times with BG11 or BG11$_0$ medium without antibiotics, and incubated for 18 h in the same medium under culture conditions. Cells were harvested, washed, and resuspended in the corresponding growth medium supplemented with 10 mM HEPES-NaOH buffer (pH 7, unless indicated otherwise), and 1 mM the indicated sugar in the experiment depicted in Fig. 3. Assays of uptake were started by addition of esculin hydrate (Sigma-Aldrich) at 100 μM, and suspensions were incubated at 30°C in the light (~170 μmol photons m^{-2} s^{-1}) for up to 70 min. One-ml samples were withdrawn and filtered. Cells on the filters were washed with 10 mM HEPES-NaOH buffer of the same pH used in the assay and were resuspended in 2 ml of 10 mM HEPES-NaOH buffer (pH 7). Fluorescence of the resulting cell suspension was measured in a Varian Cary eclipse fluorescence spectrophotometer (excitation, 360 $\pm$ 10 nm; emission, 462 $\pm$ 10 nm). Esculin solutions in the same buffer (pH 7) were used as standards. Significance in the differences of uptake between strains (as well as in other parameters investigated in this work) was assessed by unpaired Student's *t* tests, assuming a normal distribution of the data. Data sets with *P* values of <0.05 are considered significant.

Growth curves and nitrogenase activity. The growth rate constant ($\mu = [\ln 2]/t_d$, where t_d is the doubling time) was calculated from the increase in the optical density at 750 nm (OD_{750}) of shaken liquid cultures. Cultures were inoculated with an amount of cells giving an OD_{750} of about 0.05 (light path, 1 cm) and grew logarithmically until reaching an OD_{750} of about 0.8 to 0.9. The suspensions of filaments were carefully homogenized with a pipette before taking the samples.

For determination of nitrogenase activity, filaments grown in BG11 medium were harvested, washed with BG11$_0$ medium, and resuspended in BG11$_0$ medium. After 48 h of incubation under growth conditions, the filaments were used in acetylene reduction assays performed under oxic or anoxic conditions at 30°C in the light (ca. 150 μmol photons m^{-2} s^{-1}). For these assays, the cell suspensions (2 ml; ca. 10 μg Chl ml^{-1}) were placed in flasks sealed with rubber stoppers (total volume, 12 to 14 ml). For the anoxic assays, the cell suspensions were supplemented with 10 μM 3-(3,4-dichlorophenyl)-1,1-dimethylurea (DCMU), bubbled thoroughly with argon for 3 min, and incubated for 60 min under assay conditions before starting the reaction. Production of ethylene, determined by gas chromatography in

1-ml samples from the gas phase, was monitored for up to 3 h after starting the reaction by addition of acetylene (2 ml).

Light, confocal, and fluorescence microscopy. Cultures were routinely observed by light microscopy. To stain the polysaccharide layer of heterocysts, cell suspensions were mixed (1:2) with a filtered 1% (wt/vol) alcian blue (Sigma) solution.

For visualization by confocal microscopy of filaments of strains producing genetic fusions to GFP, small blocks of agar-solidified BG11 or $BG11_0$ medium bearing the filaments were excised and placed in a sample holder with a glass coverslip on top. GFP fluorescence was visualized using a Leica HCX Plan Apo 63× 1.4-numeric-aperture (NA) oil immersion objective attached to a Leica TCS SP2 confocal laser-scanning microscope. GFP was excited using 488-nm irradiation from an argon ion laser. Fluorescent emission was monitored by collection across windows of 498 to 541 nm (GFP imaging) and 630 to 700 nm (cyanobacterial autofluorescence). GFP fluorescence intensity was analyzed using ImageJ 1.45s software. To determine the relative fluorescence intensity in different cell zones, integrated density was recorded in squares of 0.2 to 0.8 μm^2. About 80 to 190 measurements were made for each of the lateral walls and septal areas of vegetative cells from BG11 or $BG11_0$ medium, and 50 to 60 measurements were made for lateral walls of heterocysts. We could not accurately quantify GFP fluorescence from heterocyst-vegetative cell septa, which are thinner than the septa between vegetative cells. Because fluorescence did not follow a normal distribution, data are presented as median and interquartile ranges (66).

For fluorescence microscopy, filaments of cells were imaged using a Leica DM6000B fluorescence microscope and an ORCA-ER camera (Hamamatsu). GFP fluorescence was monitored using a fluorescein isothiocyanate (FITC) L5 filter (excitation band pass [BP], 480/40 nm; emission BP, 527/30 nm), and red autofluorescence was monitored using a Texas red TX2 filter (excitation BP, 560/40 nm; emission BP, 645/75 nm).

Immunolocalization of SepJ. Cells from 1.5 ml of liquid cultures were collected by centrifugation, placed atop a poly-L-lysine-precoated microscope slide, and covered with a 45-μm-pore-size Millipore filter. The filter was removed and the slide was left to dry at room temperature, immersed in 70% ethanol at −20°C for 30 min, and dried for 15 min at room temperature. The cells were washed twice (2 min each time, room temperature) by covering the slide with PBS-T (PBS supplemented with 0.05% Tween 20). Subsequently, the slides were treated with a blocking buffer (5% milk powder in PBS-T) for 15 min. Cells on the slides were then incubated for 90 min with anti-SepJ-CC antibodies (17) diluted in blocking buffer (1:250), washed three times with PBS-T, incubated for 45 min in the dark with anti-rabbit antibody conjugated to FITC (1:500 dilution in PBS-T; Sigma), and washed three times with PBS-T. After being dried, several drops of FluorSave (Calbiochem) were added atop, covered with a coverslip, and sealed with nail lacquer. Fluorescence was monitored as described above, and images were analyzed with ImageJ software (http://imagej.nih.gov/ij).

Visualization of nanopores by electron microscopy. The murein sacculi (which are made of peptidoglycan) were isolated from filaments grown in BG11 medium and analyzed as described previously (18, 19). The purified sacculi were deposited on Formvar/carbon film-coated copper grids and stained with 1% (wt/vol) uranyl acetate. All of the samples were examined with a Zeiss Libra 120 Plus electron microscope at 120 kV.

FRAP analysis. For assays of intercellular transfer of esculin, filaments were harvested, resuspended in 500 μl of fresh growth medium, mixed with 15 μl of saturated (~5 mM) aqueous esculin hydrate solution, incubated for 1 h in the dark with gentle shaking at 30°C, and then washed three times with growth medium, followed by incubation in the dark for 15 min in 1 ml medium at 30°C with gentle shaking. Cells were then washed and spotted onto a BG11 or $BG11_0$ agar plate (1%, wt/vol), and excess medium was removed. Small blocks of agar with cells adsorbed on the surface were placed in a custom-built temperature-controlled sample holder under a glass coverslip at 30°C. Cells were visualized with a laser-scanning confocal microscope (Leica TCS SP5) using a Leica HCX Plan Apo 63× 1.4-NA oil-immersion objective. Fluorescence was excited at 355 nm, with detection of esculin at 443 to 490 nm and detection of Chl at 670 to 720 nm. High-resolution imaging used a 6× line average with an optical section of ~0.7 μm. FRAP measurements were without line averaging and with a wide pinhole, giving an optical section of ~4 μm. After capturing a prebleach image, the fluorescence of a defined region of interest was bleached out by scanning this region at ~6× higher laser intensity, and recovery was then recorded in a sequence of full-frame images.

For calcein and 5-CF transfer assays, calcein and 5-CF staining and FRAP analysis were performed as previously reported (7, 14). Cell suspensions were spotted onto agar and placed in a custom-built temperature-controlled sample holder with a glass coverslip on top. All measurements were carried out at 30°C. For both calcein and 5-CF, cells were imaged with a Leica HCX Plan Apo 63×, 1.4-NA oil immersion objective attached to a Leica TCS SP5 confocal laser-scanning microscope as previously described for calcein (7), with a 488-nm line argon laser as the excitation source. Fluorescent emission was monitored by collection across windows of 500 to 520 nm or 500 to 527 nm in different experiments and a 150-μm pinhole. After an initial image was recorded, the bleach was carried out by an automated FRAP routine which switched the microscope to X scanning mode, increased the laser intensity by a factor of 10, and scanned a line across one cell for 0.137 s before reducing the laser intensity, switching back to XY imaging mode, and recording a sequence of images typically at 1-s intervals.

For FRAP data analysis, we quantified kinetics of transfer of the fluorescent tracer to either (i) a terminal cell (with one cell junction) or (ii) a cell somewhere in the middle of a filament (i.e., with two cell junctions). For the first option, the recovery rate constant, R, was calculated from the formula $C_B = C_0 + C_R(1 - e^{-Rt})$, where C_B is fluorescence in the bleached cell, C_0 is fluorescence immediately after the bleach and tending toward ($C_0 + C_R$) after fluorescence recovery, t is time, and R is the recovery rate

constant due to transfer of the tracer from one neighbor cell (14). For the second option, the formula $C_B = C_0 + C_R (1 - e^{-2Rt})$ was used. Development of equations for FRAP analysis is described in the supplemental material (Text S1).

BACTH strain construction and assays. The possible interaction of the different glucoside transporters with SepJ was tested using bacterial adenylate cyclase two-hybrid (BACTH) analysis. For this analysis, all tested genes were amplified using *Anabaena* DNA as the template. The following primers were used: alr4781-7 and alr4781-8 to amplify *glsC*, all0261-7 and all0261-8 to amplify *glsP*, and all1711-9 and all1711-10 to amplify *hepP*. The PCR products were cloned in vector pSpark I, transformed into *E. coli* DH5α, and sequenced. Inserts with the correct sequence were transferred as XbaI- and KpnI-digested fragments to pUT18, pUT18C, pKNT25, and pKT25 (37), producing fusions to the 5′ and 3′ ends of the genes encoding the adenylate cyclase T18 and T25 fragments, respectively. The resulting plasmids were transformed into *E. coli* XL1-Blue to amplify the plasmids. Fusions of the *sepJ* gene to the 5′ end of T18 or T25 were as previously described (15). Isolated plasmids were cotransformed into *E. coli* BTH101 (*cya-99*). Transformants were plated onto LB medium containing selective antibiotics and 1% glucose. Efficiencies of interactions between different hybrid proteins were quantified by measurement of β-galactosidase activity in cells from liquid cultures.

To determine β-galactosidase activity, bacteria were grown in LB medium in the presence of 0.5 mM isopropyl-β-D-thiogalactopyranoside (IPTG) and appropriate antibiotics at 30°C for 16 h. Before the assays, cultures were diluted 1:5 into buffer Z (60 mM Na_2HPO_4, 40 mM NaH_2PO_4, 10 mM KCl, and 1 mM $MgSO_4$). To permeabilize cells, 30 μl of toluene and 35 μl of a 0.1% SDS solution were added to 2.5 ml of bacterial suspension. The tubes were vortexed for 10 s and incubated with shaking at 37°C for 30 min for evaporation of toluene. For the enzymatic reaction, 875 μl of permeabilized cells was added to buffer Z supplemented with β-mercaptoethanol (25 mM final concentration) to a final volume of 3.375 ml. The tubes were incubated at 30°C in a water bath for at least 5 min. The reaction was started by adding 875 μl of 0.4 mg ml^{-1} *o*-nitrophenol-β-galactoside (ONPG) in buffer Z. Samples of 1 ml, taken at different times (up to 12 min), were added to 0.5 ml of 1 M Na_2CO_3 to stop the reaction. A_{420} was recorded, and the amount of *o*-nitrophenol produced was calculated using an extinction coefficient, ε_{420}, of 4.5 mM^{-1} cm^{-1} and referred to the amount of total protein, determined by a modified Lowry procedure.

SUPPLEMENTAL MATERIAL

Supplemental material for this article may be found at https://dx.doi.org/10.1128/JB.00876-16.

TEXT S1, PDF file, 8.4 MB.

ACKNOWLEDGMENTS

We thank Antonia Herrero (Seville, Spain) for useful discussions, Alexandra Johnson (East Lansing, MI) for her cloning work related to generation of DR3912a and DR3915, and Sergio Camargo (Seville, Spain) for help with the immunofluorescence and RT-qPCR analyses.

M.N.-M. was the recipient of an FPU (Formación de Profesorado Universitario) fellowship/contract from the Spanish government. Work in Seville was supported by grant no. BFU2014-56757-P from Plan Nacional de Investigación, Spain, cofinanced by the European Regional Development Fund. Work in East Lansing was supported by the Biosciences Division, Office of Basic Energy Sciences, Office of Science, U.S. Department of Energy (grant DOE FG02-91ER20021).

REFERENCES

1. Flores E, Herrero A. 2014. The cyanobacteria: morphological diversity in a photoautotrophic lifestyle. Perspect Phycol 1:63–72. https://doi.org/10.1127/pip/2014/0008.
2. Wolk CP. 1996. Heterocyst formation. Annu Rev Genet 30:59–78. https://doi.org/10.1146/annurev.genet.30.1.59.
3. Wolk CP, Ernst A, Elhai J. 1994. Heterocyst metabolism and development, p 769–823. *In* Bryant DA (ed), The molecular biology of cyanobacteria. Kluwer Academic Publishers, Dordrecht, the Netherlands.
4. Herrero A, Stavans J, Flores E. 2016. The multicellular nature of filamentous heterocyst-forming cyanobacteria. FEMS Microbiol Rev 40:831–854. https://doi.org/10.1093/femsre/fuw029.
5. Flores E, Herrero A, Wolk CP, Maldener I. 2006. Is the periplasm continuous in filamentous multicellular cyanobacteria? Trends Microbiol 14:439–443. https://doi.org/10.1016/j.tim.2006.08.007.
6. Mariscal V, Herrero A, Flores E. 2007. Continuous periplasm in a filamentous, heterocyst-forming cyanobacterium. Mol Microbiol 65:1139–1145. https://doi.org/10.1111/j.1365-2958.2007.05856.x.
7. Mullineaux CW, Mariscal V, Nenninger A, Khanum H, Herrero A, Flores E, Adams DG. 2008. Mechanism of intercellular molecular exchange in heterocyst-forming cyanobacteria. EMBO J 27:1299–1308. https://doi.org/10.1038/emboj.2008.66.
8. Mariscal V. 2014. Cell-cell joining proteins in heterocyst-forming cyanobacteria, p 293–304. *In* Flores E, Herrero A (ed), The cell biology of cyanobacteria. Caister Academic Press, Norfolk, United Kingdom.
9. Mullineaux CW, Nürnberg DJ. 2014. Tracing the path of a prokaryotic paracrine signal. Mol Microbiol 94:1208–1212. https://doi.org/10.1111/mmi.12851.
10. Flores E, Herrero A, Forchhammer K, Maldener I. 2016. Septal junctions in filamentous heterocyst-forming cyanobacteria. Trends Microbiol 24:79–82. https://doi.org/10.1016/j.tim.2015.11.011.
11. Erickson RO. 1986. Symplastic growth and symplasmic transport. Plant Physiol 82:1153. https://doi.org/10.1104/pp.82.4.1153.
12. Flores E, Pernil R, Muro-Pastor AM, Mariscal V, Maldener I, Lechno-Yossef S, Fan Q, Wolk CP, Herrero A. 2007. Septum-localized protein required

for filament integrity and diazotrophy in the heterocyst-forming cyanobacterium *Anabaena* sp. strain PCC 7120. J Bacteriol 189:3884–3890. https://doi.org/10.1128/JB.00085-07.
13. Merino-Puerto V, Mariscal V, Mullineaux CW, Herrero A, Flores E. 2010. Fra proteins influencing filament integrity, diazotrophy and localization of septal protein SepJ in the heterocyst-forming cyanobacterium *Anabaena* sp. Mol Microbiol 75:1159–1170. https://doi.org/10.1111/j.1365-2958.2009.07031.x.
14. Merino-Puerto V, Schwarz H, Maldener I, Mariscal V, Mullineaux CW, Herrero A, Flores E. 2011. FraC/FraD-dependent intercellular molecular exchange in the filaments of a heterocyst-forming cyanobacterium, Anabaena sp. Mol Microbiol 82:87–98. https://doi.org/10.1111/j.1365-2958.2011.07797.x.
15. Ramos-León F, Mariscal V, Frías JE, Flores E, Herrero A. 2015. Divisome-dependent subcellular localization of cell-cell joining protein SepJ in the filamentous cyanobacterium *Anabaena*. Mol Microbiol 96:566–580. https://doi.org/10.1111/mmi.12956.
16. Rudolf M, Tetik N, Ramos-León F, Flinner N, Ngo G, Stevanovic M, Burnat M, Pernil R, Flores E, Schleiff E. 2015. The peptidoglycan-binding protein SjcF1 influences septal junction function and channel formation in the filamentous cyanobacterium *Anabaena*. mBio 6(4):e00376-15.
17. Mariscal V, Herrero A, Nenninger A, Mullineaux CW, Flores E. 2011. Functional dissection of the three-domain SepJ protein joining the cells in cyanobacterial trichomes. Mol Microbiol 79:1077–1088. https://doi.org/10.1111/j.1365-2958.2010.07508.x.
18. Nürnberg DJ, Mariscal V, Bornikoel J, Nieves-Morión M, Krauß N, Herrero A, Maldener I, Flores E, Mullineaux CW. 2015. Intercellular diffusion of a fluorescent sucrose analog via the septal junctions in a filamentous cyanobacterium. mBio 6(2):e02109.
19. Lehner J, Berendt S, Dörsam B, Pérez R, Forchhammer K, Maldener I. 2013. Prokaryotic multicellularity: a nanopore array for bacterial cell communication. FASEB J 27:2293–2230. https://doi.org/10.1096/fj.12-225854.
20. Omairi-Nasser A, Mariscal V, Austin JR, II, Haselkorn R. 2015. Requirement of Fra proteins for communication channels between cells in the filamentous nitrogen-fixing cyanobacterium *Anabaena* sp. PCC 7120. Proc Natl Acad Sci U S A 112(32):E4458–E4464.
21. Schilling N, Ehrnsperger K. 1985. Cellular differentiation of sucrose metabolism in *Anabaena variabilis*. Z Naturforsch 40c:776–779.
22. Curatti L, Flores E, Salerno G. 2002. Sucrose is involved in the diazotrophic metabolism of the heterocyst-forming cyanobacterium *Anabaena* sp. FEBS Lett 513:175–178. https://doi.org/10.1016/S0014-5793(02)02283-4.
23. López-Igual R, Flores E, Herrero A. 2010. Inactivation of a heterocyst-specific invertase indicates a principal role of sucrose catabolism in the heterocysts of *Anabaena* sp. J Bacteriol 192:5526–5533. https://doi.org/10.1128/JB.00776-10.
24. Vargas WA, Nishi CN, Giarrocco LE, Salerno GL. 2011. Differential roles of alkaline/neutral invertases in *Nostoc* sp. PCC 7120: Inv-B isoform is essential for diazotrophic growth. Planta 233:153–162.
25. Kolman MA, Nishi CN, Perez-Cenci M, Salerno GL. 2015. Sucrose in cyanobacteria: from a salt-response molecule to play a key role in nitrogen fixation. Life (Basel) 5:102–126.
26. Nieves-Morión M, Mullineaux CW, Flores E. 2017. Molecular diffusion through cyanobacterial septal junctions. mBio 8:e01756-16.
27. Stebegg R, Wurzinger B, Mikulic M, Schmetterer G. 2012. Chemoheterotrophic growth of the cyanobacterium *Anabaena* sp. strain PCC 7120 dependent on a functional cytochrome *c* oxidase. J Bacteriol 194:4601–4607. https://doi.org/10.1128/JB.00687-12.
28. Gora PJ, Reinders A, Ward JM. 2012. A novel fluorescent assay for sucrose transporters. Plant Methods 8:13. https://doi.org/10.1186/1746-4811-8-13.
29. Park J-J, Lechno-Yossef S, Wolk CP, Vieille C. 2013. Cell-specific gene expression in *Anabaena variabilis* grown phototrophically, mixotrophically and heterotrophically. BMC Genomics 14:759. https://doi.org/10.1186/1471-2164-14-759.
30. Kaneko T, Nakamura Y, Wolk CP, Kuritz T, Sasamoto S, Watanabe A, Iriguchi M, Ishikawa A, Kawashima K, Kimura T, Kishida Y, Kohara M, Matsumoto M, Matsuno A, Muraki A, Nakazaki N, Shimpo S, Sugimoto M, Takazawa M, Yamada M, Yasuda M, Tabata S. 2001. Complete genomic sequence of the filamentous nitrogen-fixing cyanobacterium *Anabaena* sp. strain PCC 7120. DNA Res 8:205–213. https://doi.org/10.1093/dnares/8.5.205.
31. Elhai J, Wolk CP. 1988. A versatile class of positive-selection vectors based on the nonviability of palindrome-containing plasmids that allows cloning into long polylinkers. Gene 68:119–138. https://doi.org/10.1016/0378-1119(88)90605-1.
32. Cui J, Davidson AL. 2011. ABC solute importers in bacteria. Essays Biochem 50:85–99. https://doi.org/10.1042/bse0500085.
33. López-Igual R, Lechno-Yossef S, Fan Q, Herrero A, Flores E, Wolk CP. 2012. A major facilitator superfamily protein, HepP, is involved in formation of the heterocyst envelope polysaccharide in the cyanobacterium Anabaena sp. strain PCC 7120. J Bacteriol 194:4677–4687. https://doi.org/10.1128/JB.00489-12.
34. Drew D, Sjöstrand D, Nilsson J, Urbig T, Chin CN, de Gier JW, von Heijne G. 2002. Rapid topology mapping of *Escherichia coli* inner-membrane proteins by prediction and PhoA/GFP fusion analysis. Proc Natl Acad Sci U S A 99:2690–2695. https://doi.org/10.1073/pnas.052018199.
35. McKinney RE. 1953. Staining bacterial polysaccharides. J Bacteriol 66:453–454.
36. Karimova G, Pidoux J, Ullmann A, Ladant D. 1998. A bacterial two-hybrid system based on a reconstituted signal transduction pathway. Proc Natl Acad Sci U S A 95:5752–5756. https://doi.org/10.1073/pnas.95.10.5752.
37. Battesti A, Bouveret E. 2012. The bacterial two-hybrid system based on adenylate cyclase reconstitution in Escherichia coli. Methods 58:325–334. https://doi.org/10.1016/j.ymeth.2012.07.018.
38. Stynen B, Tournu H, Tavernier J, Van Dijck P. 2012. Diversity in genetic in vivo methods for protein-protein interaction studies: from the yeast two-hybrid system to the mammalian split-luciferase system. Microbiol Mol Biol Rev 76:331–382. https://doi.org/10.1128/MMBR.05021-11.
39. Flaherty BL, van Nieuwerburgh F, Head SR, Golden JW. 2011. Directional RNA deep sequencing sheds new light on the transcriptional response of *Anabaena* sp. strain PCC 7120 to combined-nitrogen deprivation. BMC Genomics 12:332. https://doi.org/10.1186/1471-2164-12-332.
40. Nicolaisen K, Mariscal V, Bredemeier R, Pernil R, Moslavac S, López-Igual R, Maldener I, Herrero A, Schleiff E, Flores E. 2009. The outer membrane is a permeability barrier for intercellularly exchanged metabolites in a heterocyst-forming cyanobacterium. Mol Microbiol 74:58–70. https://doi.org/10.1111/j.1365-2958.2009.06850.x.
41. Reinders A, Sivitz AB, Ward JM. 2012. Evolution of plant sucrose uptake transporters. Front Plant Sci 3:22.
42. Stuart RK, Mayali X, Lee JZ, Craig Everroad R, Hwang M, Bebout BM, Weber PK, Pett-Ridge J, Thelen MP. 2015. Cyanobacterial reuse of extracellular organic carbon in microbial mats. ISME J 10:1240–1251.
43. Rippka R, Deruelles J, Waterbury JB, Herdman M, Stanier RY. 1979. Generic assignments, strain histories and properties of pure cultures of cyanobacteria. J Gen Microbiol 111:1–61.
44. Ungerer JL, Pratte BS, Thiel T. 2008. Regulation of fructose transport and its effect on fructose toxicity in *Anabaena* spp. J Bacteriol 190:8115–8125. https://doi.org/10.1128/JB.00886-08.
45. Ayre BG. 2011. Membrane-transport systems for sucrose in relation to whole-plant carbon partitioning. Mol Plant 4:377–394. https://doi.org/10.1093/mp/ssr014.
46. Escudero L, Mariscal V, Flores E. 2015. Functional dependence between septal protein SepJ from *Anabaena* sp. strain PCC 7120 and an amino acid ABC-type uptake transporter. J Bacteriol 197:2721–2730. https://doi.org/10.1128/JB.00289-15.
47. Yang DC, Peters NT, Parzych KR, Uehara T, Markovski M, Bernhardt TG. 2011. An ATP-binding cassette transporter-like complex governs cell-wall hydrolysis at the bacterial cytokinetic ring. Proc Natl Acad Sci U S A 108:E1052–E1060. https://doi.org/10.1073/pnas.1107780108.
48. Bartual SG, Straume D, Stamsås GA, Muñoz IG, Alfonso C, Martínez-Ripoll M, Håvarstein LS, Hermoso JA. 2014. Structural basis of PcsB-mediated cell separation in *Streptococcus pneumoniae*. Nat Commun 5:3842.
49. Domínguez-Cuevas P, Porcelli I, Daniel RA, Errington J. 2013. Differentiated roles for MreB-actin isologues and autolytic enzymes in *Bacillus subtilis* morphogenesis. Mol Microbiol 89:1084–1098. https://doi.org/10.1111/mmi.12335.
50. Meisner J, Montero Llopis P, Sham LT, Garner E, Bernhardt TG, Rudner DZ. 2013. FtsEX is required for CwlO peptidoglycan hydrolase activity during cell wall elongation in *Bacillus subtilis*. Mol Microbiol 89:1069–1083. https://doi.org/10.1111/mmi.12330.
51. Schlösser A, Kampers T, Schrempf H. 1997. The *Streptomyces* ATP-binding component MsiK assists in cellobiose and maltose transport. J Bacteriol 179:2092–2095. https://doi.org/10.1128/jb.179.6.2092-2095.1997.
52. Webb AJ, Homer KA, Hosie AH. 2008. Two closely related ABC transporters in *Streptococcus mutans* are involved in disaccharide and/or oligo-

saccharide uptake. J Bacteriol 190:168–178. https://doi.org/10.1128/JB.01509-07.
53. Ferreira MJ, de Sá-Nogueira I. 2010. A multitask ATPase serving different ABC-type sugar importers in *Bacillus subtilis*. J Bacteriol 192:5312–5318. https://doi.org/10.1128/JB.00832-10.
54. Watanabe A, Hiraga K, Suda M, Yukawa H, Inui M. 2015. Functional characterization of *Corynebacterium alkanolyticum* β-xylosidase and xyloside ABC transporter in *Corynebacterium glutamicum*. Appl Environ Microbiol 81:4173–4183. https://doi.org/10.1128/AEM.00792-15.
55. Pernil R, Picossi S, Mariscal V, Herrero A, Flores E. 2008. ABC-type amino acid uptake transporters Bgt and N-II of *Anabaena* sp. strain PCC 7120 share an ATPase subunit and are expressed in vegetative cells and heterocysts. Mol Microbiol 67:1067–1080. https://doi.org/10.1111/j.1365-2958.2008.06107.x.
56. Hu N-T, Thiel T, Giddings TH, Wolk CP. 1981. New *Anabaena* and *Nostoc* cyanophages from sewage settling ponds. Virology 114:236–246. https://doi.org/10.1016/0042-6822(81)90269-5.
57. Mackinney G. 1941. Absorption of light by chlorophyll solutions. J Biol Chem 140:315–322.
58. Ausubel FM, Brent R, Kingston RE, Moore DD, Seidman JG, Smith JA, Struhl K. 2014. Current protocols in molecular biology. Greene Publishing and Wiley-Interscience, New York, NY.
59. Elhai J, Vepritskiy A, Muro-Pastor AM, Flores E, Wolk CP. 1997. Reduction of conjugal transfer efficiency by three restriction activities of *Anabaena* sp. strain PCC 7120. J Bacteriol 179:1998–2005. https://doi.org/10.1128/jb.179.6.1998-2005.1997.
60. Cai Y, Wolk CP. 1990. Use of a conditionally lethal gene in *Anabaena* sp. strain PCC 7120 to select for double recombinants and to entrap insertion sequences. J Bacteriol 172:3138–3145. https://doi.org/10.1128/jb.172.6.3138-3145.1990.
61. Wolk CP, Cai Y, Cardemil L, Flores E, Hohn B, Murry M, Schmetterer G, Schrautemeier B, Wilson R. 1988. Isolation and complementation of mutants of *Anabaena* sp. strain PCC 7120 unable to grow aerobically on dinitrogen. J Bacteriol 170:1239–1244. https://doi.org/10.1128/jb.170.3.1239-1244.1988.
62. Valladares A, Rodríguez V, Camargo S, Martínez-Noël GM, Herrero A, Luque I. 2011. Specific role of the cyanobacterial PipX factor in the heterocysts of *Anabaena* sp. strain PCC 7120. J Bacteriol 193:1172–1182. https://doi.org/10.1128/JB.01202-10.
63. Black TA, Cai Y, Wolk CP. 1993. Spatial expression and autoregulation of *hetR*, a gene involved in the control of heterocyst development in *Anabaena*. Mol Microbiol 9:77–84. (Erratum, **10:**1153, 1993).
64. Cormack BP, Valdivia RH, Falkow S. 1996. FACS-optimized mutants of the green fluorescent protein (GFP). Gene 173:33–38. https://doi.org/10.1016/0378-1119(95)00685-0.
65. Livak KJ, Schmittgen TD. 2001. Analysis of relative gene expression data using real-time quantitative PCR and the 2(-Delta Delta C(T)) method. Methods 25:402–408. https://doi.org/10.1006/meth.2001.1262.
66. Krzywinski M, Altman N. 2014. Visualizing samples with box plots. Nat Methods 11:119–120. https://doi.org/10.1038/nmeth.2813.